# Fault Tolerance Algorithm of Steering Actuator in Three-Wheeled Electric Mobility Based on Model Predictive Control


1st Jung Hyun Choi
*Depart. of-*
*Robotics Engineering*
*DGIST*
Daegu, South Korea
jhchoi-sog@dgist.ac.kr

2nd Hiroshi Fujimoto
*Graduate School of-*
*Frontier Sciences*
*The University of Tokyo*
Kashiwa, Chiba, Japan
fujimoto@k.u-tokyo.ac.jp

3rd Sehoon Oh
*Depart. of-*
*Robotics Engineering*
*DGIST*
Daegu, South Korea
sehoon@dgist.ac.kr



IECON 2021 - 47th Annual Conference of the IEEE Industrial Electronics Society | 978-1-6654-3554-3/21/$31.00 ©2021 IEEE | DOI: 10.1109/IECON48115.2021.9589729



***Abstract*—Three-wheeled electric mobility is an effective means of transport in a small and narrow space. As this electric mobility is widely utilized, the request of safety and performance for this mobility has become important. And thus a fault tolerance function needs to be developed to minimize the user's intervention and improve driving performance. Fault-tolerance technology is applied mainly to sensors, but a fault tolerance function is also required from the viewpoint of driving-related actuators.**

**In this paper, a fault tolerance algorithm is proposed taking use of newly-proposed concept steering fault disturbance and Model Predictive Control (MPC).**

**To this end, an index is proposed to represent the failure of the steering motor as an objective numerical value, and this index is used for the driving controller of electric mobility.**

**In this driving controller, MPC is designed based on a dynamic model of three-wheeled electric mobility to regulate the input values of steering angle and yaw moment to maintain driving performance by referring to the proposed index.**

**By using the proposed algorithm based on the MPC, electric mobility can drive along a given route without user's intervention in the event of a breakdown. The proposed fault tolerance algorithm is verified through various driving scenarios using a simulation model that reflects three-wheeled electric mobility.**



***Index Terms*—fault tolerance, steering system, electric mobility, model predictive control**


## I. Introduction

Electric mobility systems are used for a variety of purposes, including robots for guidance [1] delivery [2], and warehouse logistics [3], [4], as well as personal mobility. The driving environment of such electric mobility is often operated in a narrow space or crowded space than in a wide vacant lot or road. For this reason, small-sized electric mobility is required and a three-wheeled structure is widely adopted for this electric mobility.

Another driving environment of such electric mobility is a space that is cumbersome and difficult for workers. In such a space, electric mobility is developed to reduce the labor of direct work and protect workers, so it is often operated as autonomous driving. that does not require worker's intervention. Therefore, in electric mobility of autonomous driving that requires minimal human intervention, a fault tolerance function capable of coping with errors in electric internal functions is required to increase safety and work efficiency.

There are many ways to realize fault tolerance, which is widely used in electric mobility when a fault occurs in the function of the sensor [5], [6].

In addition to the sensor field, the fault tolerance in the driving/steering system is required to ensure the function of driving in electric mobility. However, unlike sensors, adding more extra motors to the system is not suitable in terms of cost and complexity of the system. Fortunately, most electric mobility consist of redundant driving system in which the number of the actuators is more than the degrees of freedom of motion. Taking advantage of this, many studies are being conducted in the field of electric vehicles to maintain the original driving function by combining the functions of other driving motors even if one motor fails [7]–[9].

On the other hand, the fault of the steering system is difficult to handle since the number of actuator is less and the mechanism is more complicated than the driving system. Moreover, a steering system fault has a greater adverse effect on the electric mobility than a driving system fault.

Therefore, a method to overcome the fault by using the driving resources in the existing system without installing an extra motors is required when a fault occurs on the steering system.

There are studies on attempts to directly manipulate the steering angle of a vehicle by using the driving torque of the vehicle when the steering motor fails [10]. This method uses the scrub radius determined by the geometrical installation angle of the wheel (Kingpin angle). Driving force is applied to this scrub radius to generate the steering torque of each wheel. This study is a successful case of fault tolerance realization by using the structural characteristics of the steering system. However, this cannot be applied to electric mobility with a completely different steering structure, such as three-wheeled electric mobility without a kingpin angle.

There is also research related to fault tolerance of the three-wheeled system [11]. However, this approach focused on how

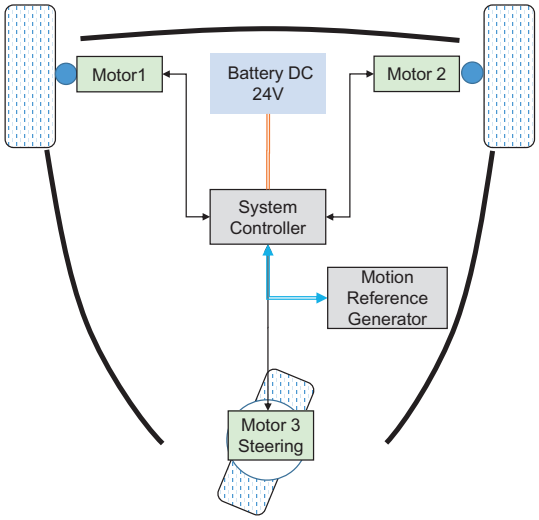


Fig. 1. Schematic of three-wheeled electric mobility including the steering system

to diagnose a failure situation in a three-wheeled mobile robot, and the purpose of this diagnose was to stop the operation of the robot to avoid additional malfunctions when a failure situation occurs.

In spite of the high demand for the three-wheeled electric mobility, the development of fault tolerance technology that reflects the structural characteristics of three-wheeled electric mobility still needs intensive research works.

Therefore, fault tolerance technology is needed to maintain driving performance (or autonomous driving) and minimize user intervention even in the event of a wheeled vehicle failure.

In this study, we propose a fault tolerance algorithm that can overcome the steering system fault and keep a given driving command in three-wheel electric mobility. This algorithm utilizes the existing driving actuator of the electric mobility to overcome the steering failure. In addition, an index that numerically represents a fault state of the steering system is proposed. This index considered as a disturbance of the steering system. Taking account of this index, Model Predictive Control (MPC) is designed to maintain the given driving trajectory without additional process such as human intervention or manual switching control input to dealt with the steering failure .

The structure of this paper is as follows. In Section II, characteristics and dynamic analysis of three-wheel electric mobility are performed. In Section III, an index that numerically represents the fault state of the steering system in three-wheel electric mobility is proposed. Base on this index, MPC is designed, which contains the method of changing the input source from the steering angle to the yaw moment when the steering system fails. This fault-tolerance algorithm is verified by using a simulation that includes a driving model of electric mobility in Section IV. Finally, the conclusion and discussion are in Section V.

TABLE I
SPECIFICATIONS OF THE ELECTRIC MOBILITY

| | |
|---|---|
| Real-time controller | cRIO (National Instruments) |
| Motor driver | Gold Solo Whistle (Elmo) |
| Gyro sensor | Pmod Gyro (Digilent) |
| Front Wheel | TM90-04-K, 400W, DC24V (TM Tech-I) |
| Steering | EC-i 52, 180W, DC24V (Maxon) |
| Weight $M$ | 500 kg |
| Distance from CG-Front wheel $l_f$ | 0.532 m |
| Distance from CG-Rear wheel $l_r$ | 0.653m |
| Tire radious $r_w$ | 0.0125m |
| Distance between Front wheels $l_w$ | 0.626m |

## II. DYNAMIC MODEL OF THREE-WHEELED ELECTRIC MOBILITY

In this section, the structure of three-wheeled electric mobility is introduced to explain its components and their functions including steering system. Then, the dynamic analysis of the three-wheeled electric mobility is elaborated in detail.

### A. Overview of the three-wheeled Electric Mobility

The structure of the electric mobility introduced in this study is shown in Fig. 1. In the detailed structure, the electric mobility is composed of 3 wheels, which are two driving motors and one steering motor. This structure is different from other three-wheeled electric mobility that has only a passive caster without a separate steering motor.

Since the electric mobility with passive casters cannot directly generate the steering angle for turning, the yaw rate is generated only by using the yaw moment of the chassis, which leads to the steering angle of the passive caster wheel. In this mechanism, the steering angle of the caster wheel is determined according to the turning characteristics of the driving dynamics. Notes that the yaw moment acting on the chassis is generated as much as the difference between driving forces generated by two driving wheels.

The disadvantage of this type of steering is the inefficiency of the driving force, which means that additional driving forces are required to steer the chassis. Therefore, a steering motor is necessary for a three-wheeled structure in order to fully utilize the torque of the driving motor as a driving force. In other words, electric mobility with a steering motor has redundancy (steering motor and the difference between two driving forces) to generate a yaw moment, and thus it is possible to maintain a turning operation even when one of two methodologies fails.

This paper proposes a control algorithm that can realize the fault tolerance taking advantage of these two methodologies. The detailed specifications of the electric mobility which is the target of the proposed algorithm are shown in Table I.

### B. Dynamic Analysis of Three-wheeled Mobility with Active Steering System

The dynamic analysis of the three-wheeled electric mobility is conducted to formulate the state-space equation, which is utilized to design the driving control based on fault tolerance. Fig. 2 describes the Free-Body Diagram (FBD) of the mobility which has three wheels including active steering mechanism. From this FBD, the lateral dynamics and yaw motion dynamics can be derived by referring to the fundamental vehicle dynamics [12]. The dynamic equations of the lateral motion and yaw motion are derived utilizing the lateral force $F^y$, the yaw moment $M_{in}$ as follows:

$$F^y = M\dot{v}_y = F^y_{fl} + F^y_{fr} + F^x_r \sin\delta + F^y_r \cos\delta \quad (1)$$

$$I\dot{\gamma} = 2l_r F^y_f + M_{in} \quad (2)$$

$$M_{in} = l_f F^y_r \cos\delta + \frac{1}{2}(F^x_{fr} - F^x_{fl}) + l_f F^x_r \sin\delta + F^y_r \cos\delta, \quad (3)$$

where $M$ is the mass of the whole mobility, $\delta$ is the steering angle, and $l_f$ and $l_r$ are the distances between Center of Mass (CoM) and the front wheels/ the rear wheel, respectively. $F^x_r$ is the longitudinal force with respect to the $x$-axis of the rear wheel due to the net force generated by the front wheels, and $F^y_{fl}/F^y_{fr}$ are the lateral forces with respect to the $y$-axis of the front left wheel and right wheel, respectively. Usually, it can be assumed that the left and right lateral forces on the front wheels are equal. In this paper, the longitudinal force $F^x_r$ can be ignore. Let the side slip angle $\beta$ and yaw rate $\gamma$ represent the state variables of the robot system. By using the kinematic relationship as $a_y = v_x(\dot{\beta} + \gamma)$ and assuming that $\delta$ is relatively small, (1),(2) is rewritten as follows:

$$Mv_x(\dot{\beta} + \gamma) = (2F^y_f + F^y_r) + \gamma \quad (4)$$

$$I\dot{\gamma} = (2l_f F^y_f - l_r F^y_r) \quad (5)$$

Based on (4),(5), the state equation is constructed with a side-slip angle $\beta$ and the yaw rate $\gamma$ as the state $x$ as follows. In this equation, steering angle $\delta$ and yaw moment $M_z$ are adopted as the input $u$.

$$\dot{x} = \boldsymbol{A}x + \boldsymbol{B}u \quad (6)$$

$$y = \boldsymbol{C}x \quad (7)$$

$$\boldsymbol{A} = \begin{bmatrix} \frac{(-l_f - 2C_r)}{Mv_x} & \frac{(-C_f l_f + 2C_r l_r - Mv_x^2)}{Mv_x^2} \\ \frac{(-C_f l_f + 2l_r C_r)}{I} & \frac{(-C_f l_f^2 - 2C_r l_r^2)}{Iv_x} \end{bmatrix}$$

$$\boldsymbol{B} = [\boldsymbol{B_1} \quad \boldsymbol{B_2}] = \begin{bmatrix} \frac{C_f}{Mv_x^2} & 0 \\ \frac{l_f C_f}{I} & \frac{1}{I} \end{bmatrix}$$

$$\boldsymbol{C} = [0 \quad 1]$$

where $C_f$ and $C_r$ are the cornering stiffness, $V_x$ is the vehicle speed.

## III. Driving Control Algorithm with Fault Tolerance

In this section, an index that can recognize the steering system failure is proposed, and the detailed fault tolerance algorithm including Model Predictive Control is described.

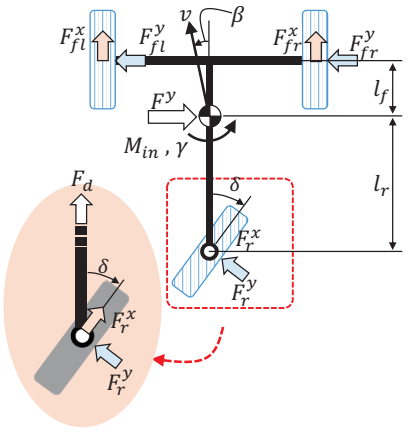


Fig. 2. Free body diagram of three-wheeled electric mobility

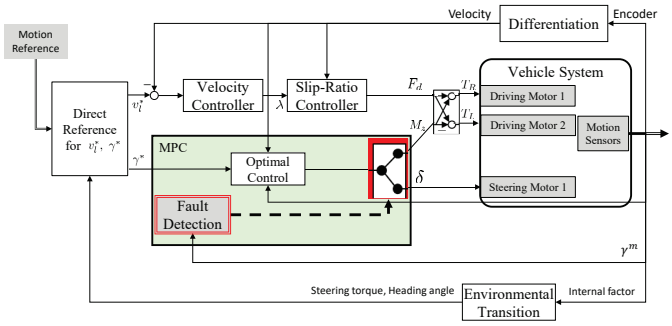


Fig. 3. Overall driving control algorithm including fault tolerance

### A. Overall Driving Control Algorithm

The entire driving control algorithm for the three-wheeled electric mobility is proposed as shown in Fig. 3. This control algorithm consists of the longitudinal motion control and a yaw motion control. First, for the longitudinal motion control, slip ratio control-based velocity control is applied such that the mobility can achieve the desired velocity.

Then, for the yaw motion controller, Model Predictive Control is applied to achieve the desired yaw rate. The cost function (8) of the proposed MPC consists of the error of the yaw rate $e^\gamma$ and two input values ($\delta$ and $M_z$) such that MPC can minimize the error while reducing the control inputs.

$$J = \int_0^\infty \left( (e^\gamma)^T \boldsymbol{Q}_\gamma e^\gamma + \delta^T \boldsymbol{R}_{\boldsymbol{\delta}} \delta + M_z^T \boldsymbol{R}_{\boldsymbol{M_z}} M_z \right) dt \quad (8)$$

Notice that two inputs $\delta$ and $M_z$ are utilized in the cost function, which are redundant in generating the yaw rate as shown in Fig. 4. The first case shows that the steering angle $\delta$ generates the yaw rate (normal driving condition), while the second case shows yaw moment $M_z$ generates the yaw rate, which can be the case when the steering motor fails (steering actuator failure). Although both inputs are included in the objective function, it is required that $\delta$ and $M_z$ should be automatically and appropriately selected based on the failure of the steering system.

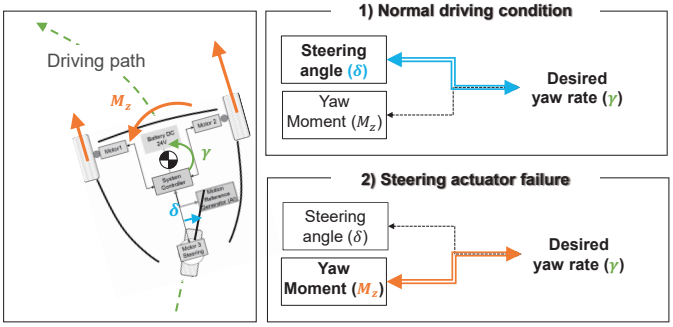


Fig. 4. Two ways to generate the yaw rate; the fundamental concept for the fault-tolerance

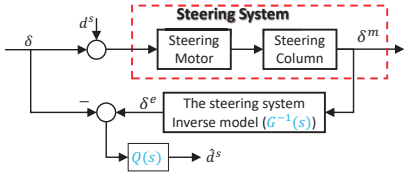


Fig. 5. Structure of steering-fault disturbance observer

For this, an algorithm that recognizes the failure situation in the system and changes the control input accordingly is needed as well as proper weighting for $\boldsymbol{R_\delta}$ and $\boldsymbol{R_{M_z}}$. The control input switching process between $\delta$ and $M_z$ in case of the steering system failure should be automatically conducted by the MPC algorithm without any involvement of users. This is considered a necessary part for autonomous driving electric mobility and is a fundamental idea in this study. To this end, a dynamic model for the steering system is derived and a failure index that expresses the failure situation numerically is proposed baesd on the derived dynamics.

### *B. Fault Index by using Steering-Fault Disturbance Observer*

In order to recognize the failure of the steering system by the algorithm itself without user intervention, an index is required that can represent the failure situation as an objective numerical value. In this study, the steering fault disturbance is proposed as an index indicating the failure situation based on the structure and dynamics of the steering system.

Fig. 5 shows the schematic model of the steering system and the concept of steering fault disturbance, where the steering system consists of the mechanical structures such as the steering motor and steering column. Notice that there is no steering wheel or driver in this model unlike general vehicles, since the target of the proposed algorithm is autonomous electric mobility. Since the steering angle of this mobility is controlled to follow the desired steering angle $\delta$, the dynamic model of this steering system from $\delta$ to the actual steering angle $\delta^m$ is considered a first-order delay system with a certain bandwidth, $\tau_\delta$ [13] as follows.

$$\delta^m = G(s)\delta = \frac{1}{\tau_\delta s + 1}\delta \tag{9}$$

TABLE II
SPECIFICATIONS OF THE ELECTRIC MOBILITY

| Weighting factor | Value | Boundary condition | Value |
|---|---|---|---|
| $Q_\gamma$ | 1e5 | $\delta_{(min,max)}$ | $\pm 1.5$ [rad] |
| $R_\delta$ | 1e1 | $M_{z,(min,max)}$ | $\pm 50$ [Nm] |
| $R_{M_z}$ | $1e-2$ | $\hat{d}^s_{(min,max)}$ | $\pm 0.01$ |

Then, a steering fault disturbance $\hat{d}^s$ can be observed by using this steering system model. The design of the disturbance observer is designed as follows.

$$\hat{d}^s = \frac{Q(s)}{G(s)}\delta^m - Q(s)\delta \tag{10}$$

where $Q(s)$ is designed as a low-pass filter.

### *C. Fault Tolerance Control Design by using MPC with the Fault Recognition Index*

The MPC is applied to change the control input when a failure occurs by using the index indicating the failure condition. For this, the cost function, linear constraint, and boundary condition are defined as follows.

$$\text{min. } \boldsymbol{Q_\gamma}\sum_{k=1}^{N} e_\gamma^2(k) + \boldsymbol{R_\delta}\sum_{k=0}^{N-1}\delta(k-1)^2 + \boldsymbol{R_{M_z}}\sum_{k=0}^{N-1} M_z(k-1)^2 \tag{11}$$

subject to

$$x(k) = \boldsymbol{A_d}x(k-1) + \boldsymbol{B_{1d}}\delta(k-1) + \boldsymbol{B_{2d}}M_z(k-1) \tag{12}$$
$$y(k) = Cx(k) \tag{13}$$
$$e_\gamma(k) = \gamma(k) - y(k) \tag{14}$$
$$\delta^e(k) = {G_d}^{-1}\delta^m(k-1) \tag{15}$$
$$\hat{d}^s(k) = \delta^e(k) - \delta(k-1) \tag{16}$$
$$\delta_{min} \le \delta(k) \le \delta_{max} \tag{17}$$
$$M_{z,min} \le M_z(k) \le M_{z,max} \tag{18}$$
$$\hat{d}^s_{min} \le \hat{d}^s(k) \le {\hat{d}^s}_{max}, \tag{19}$$

where $Q_\gamma$, $R_\delta$, and $R_{M_z}$ are the weighting factors for the error of yaw rate, steering angle, and yaw moment respectively. The $\boldsymbol{A_d}$,$\boldsymbol{B_{1d}}$, $\boldsymbol{B_{2d}}$, and $G_d$ are the discrete time models of $\boldsymbol{A}$,$\boldsymbol{B_1}$, $\boldsymbol{B_2}$, and $G$ respectively. In particular, an equality constraint of $\hat{d}^s$, $\delta^e$ is added to define the index indicating the failure condition, and the inequality constraint was also set as a condition to make this value as small as possible. In this way, in a normal driving condition, $\delta$ will mainly serve as an input value to reduce the yaw rate error, and $\hat{d}^s$ will be maintained at a value close to 0. On contrary, a fault situation occurs, $\hat{d}^s$ will increase. At this time, since $\hat{d}^s$ is set as a boundary condition, the input of steering angle still will converge to the measured steering angle.

Notice that the fault tolerance as well as the turning/rotating performance is realized through the cost function and the constraints designed above; the yaw rate error will be reduced utilizing either the steering angle $\delta$ or the yaw moment $M_z$.

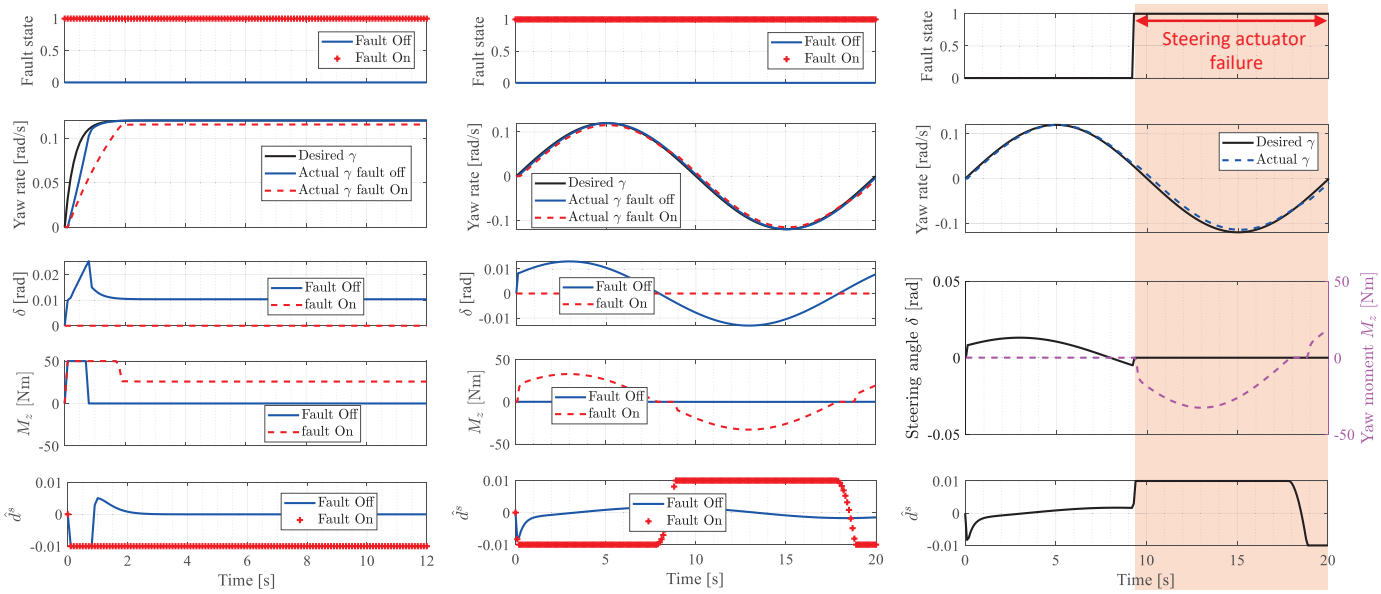


(a) (b) (c)

Fig. 6. Simulation result for fault tolerance of (a) constant gyration motion at $V_x = 15$ m/s and 0.122 rad/s (b) slalom motion at $V_x = 15$ m/s and sinusoidal yaw rate motion with 0.05 Hz (c) fault situation during slalom motion at $V_x = 15$ m/s and sinusoidal yaw rate motion with 0.05 Hz

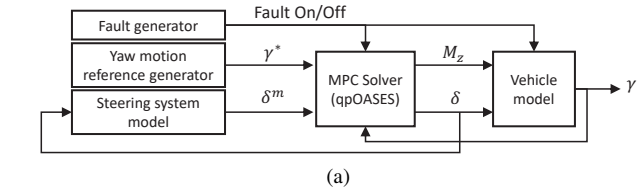


(a)

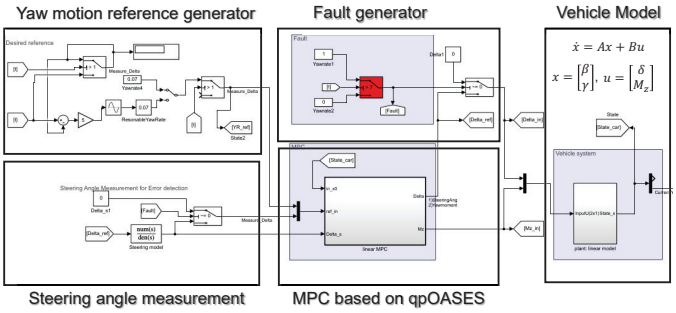


(b)

Fig. 7. (a) The block diagram of the simulation configuration. (b) The simulation model for the steering-fault tolerance by using Model Predictive Control in Matlab/Simulink with qpOASES [14]

When any fault occurs in the steering system, the yaw moment $M_z$ will increase to reduce the yaw rate error while keep the steering fault disturbance within the inequality constraint.

To obtain the optimal solution of MPC proposed in this study, qpOASES [14] is utilized and the cost function and equality/inequality constraint are transformed into a Standard QP (SQP) problem [15].

## IV. Simulation Verification

### A. Simulation Model with qpOASES

In this study, the proposed steering system failure overcoming algorithm is verified by simulation using Simulink-based qpOASES. Fig. 7 (a) shows the configuration of the simulation. Fig. 7 (b) is the model for the entire driving simulation including the electric mobility model. First, the model of electric mobility was constructed with the same dynamics equation as (6) (vehicle model part). In this simulation, the measurement steering angle, $\delta^m$ is assumed as the output measurement of the steering model (steering angle measurement part). Yaw motion reference generator is included to generate yaw rate commands to realize the turning operation of the vehicle. Fault generator also is included to simulate the actual steering system failure situation. This fault generator arbitrarily removes the normal steering angle input to the electric mobility model to cause a fault situation. The parameters applied in the MPC of this simulation are shown in Table II.

### B. Simulation Results

The fault tolerance algorithm proposed in this study is verified through several driving scenarios using the developed simulation model. Driving Scenarios are: 1) first, the mobility is controlled to realize J-turn driving path at a constant speed, then the driving performances are compared for the normal driving condition and fault situation. In the second scenario, the slalom driving path are given and the driving performances of the mobility are compared. In the third scenario, the steering system fails during the same slalom driving path as scenario 2, and the driving performance is compared with the normal driving condition. It is noted that the measured steering

angle is assumed to be zero in the failure situation due to the characteristics of the simulation model. Moreover, in all driving scenarios, the electric mobility speed is controlled to keep $V_x = 15m/s$.

The simulation results for the first scenario are shown in Fig. 6 (a). The comparison of driving performance and corresponding input values are shown in the second to the fourth subplots in Fig. 6 (a) respectively, where the red dotted lines represent the fault situation while the blue solid lines represent the normal condition. As expected, even when the steering system fails, the yaw rate depicted in the second subplot in Fig. 6 (a) shows that the function of turning driving is maintained even with the performance degradation (about $9\%$ increase in the steady-state yaw rate error compared to the normal driving condition). The yaw moment $M_z$ increases for the first 0.8 seconds even without failure, which can be attributed to the weighting $\boldsymbol{R_{Mz}}$ set in the cost function. In fact, when a fault occurs, $\delta$ is still calculated in the MPC controller and does not converge to 0. However, since the current steering system is in a faulty state, $\delta$ is useless. Therefore $\delta$ is assumed to zero in this simulation.

It should be noted that the value of $M_z$ increases appropriately when a fault condition occurs as shown in the red dashed line in the third subplot in Fig. 6 (a) in the proposed MPC, which verifies that the proposed algorithm can transfer the control input from the steering angle to the yaw moment automatically to generate the yaw rate under fault conditions.

In the second scenario, the yaw rate command value is given as a sinusoidal value for the slalom driving path as shown in Fig. 6 (b), which also shows that the proposed algorithm can transfer the control input to keep the yaw rate (with the degradation of $8\%$ steady-state error) when faults occur. It can be also verified that the estimated state fault disturbance $\hat{d}^s$ is suppressed well according to the value set in the given inequality constraint.

In the third scenario, unlike the previous two driving scenarios, a fault in the steering system occurs while slalom driving. This case is the most dangerous case, and it should be confirmed that the driving function is maintained even with this dynamic change of fault situation. To this end, the failure condition is generated in the simulation model at 8 seconds as shown in the first-row subplot in Fig. 6 (c).

The result verifies that the slalom driving function is still maintained even though the error in terms of the yaw rate slightly increases. The third subplot of Fig. 6 (c) also shows that the proposed algorithm can successfully transfer the control input as soon as a failure occurs. Steering fault disturbance $\hat{d}^s$ value rapidly increases due to the failure, but it is regulated under the boundary by the increase in $M_z$.

## V. Conclusion

In this study, a control algorithm to overcome the failure of the steering system in three-wheeled electric mobility was introduced.

This algorithm contains an index that recognizes the failure situation of electric mobility and is adopted to the algorithm to overcome the failure situation of the system. This algorithm further strengthens the function of autonomous driving and reduces the user's additional work in the fault situation.

The effectiveness of the proposed algorithm is verified through several driving scenarios. In particular, it can be seen that even in the event of a failure of the steering motor during the turning driving, the given turning driving performance is quickly recovered through the proposed algorithm by transferring the control input. In the future, the proposed algorithm should be verified by using a real vehicle model such as CarSIM or real vehicle driving.

## References


[1] R. Pinillos, S. Marcos, R. Feliz, E. Zalama, and J. Gómez-García-Bermejo, "Long-term assessment of a service robot in a hotel environment," *Robotics and Autonomous Systems*, vol. 79, pp. 40–57, 2016.

[2] Y. Dobrev, M. Vossiek, M. Christmann, I. Bilous, and P. Gulden, "Steady delivery: Wireless local positioning systems for tracking and autonomous navigation of transport vehicles and mobile robots," *IEEE Microwave Magazine*, vol. 18, no. 6, pp. 26–37, 2017.

[3] G. Li, R. Lin, M. Li, R. Sun, and S. Piao, "A master-slave separate parallel intelligent mobile robot used for autonomous pallet transportation," *Applied Sciences*, vol. 9, no. 3, p. 368, 2019.

[4] B. Horan, Z. Najdovski, T. Black, S. Nahavandi, and P. Crothers, "Oztug mobile robot for manufacturing transportation," in *2011 IEEE International Conference on Systems, Man, and Cybernetics*. IEEE, 2011, pp. 3554–3560.

[5] Z. Zhao, J. Wang, J. Cao, W. Gao, and Q. Ren, "A fault-tolerant architecture for mobile robot localization," in *2019 IEEE 15th International Conference on Control and Automation (ICCA)*. IEEE, 2019, pp. 584–589.

[6] K. Bader, B. Lussier, and W. Schön, "A fault tolerant architecture for data fusion: A real application of kalman filters for mobile robot localization," *Robotics and Autonomous Systems*, vol. 88, pp. 11–23, 2017.

[7] C. J. Ifedi, B. C. Mecrow, S. T. Brockway, G. S. Boast, G. J. Atkinson, and D. Kostic-Perovic, "Fault-tolerant in-wheel motor topologies for high-performance electric vehicles," *IEEE Transactions on Industry Applications*, vol. 49, no. 3, pp. 1249–1257, 2013.

[8] R. Wang and J. Wang, "Fault-tolerant control for electric ground vehicles with independently-actuated in-wheel motors," *Journal of Dynamic Systems, Measurement, and Control*, vol. 134, no. 2, 2012.

[9] S. Park, K. Oh, Y. Jeong, and K. Yi, "Model predictive control-based fault detection and reconstruction algorithm for longitudinal control of autonomous driving vehicle using multi-sliding mode observer," *Microsystem Technologies*, vol. 26, no. 1, pp. 239–264, 2020.

[10] K. Miyahara, H. Fujimoto, and Y. Hori, "Rear steer actuator-less four-wheel steering system for four-wheel driving electric vehicles," in *IECON 2018-44th Annual Conference of the IEEE Industrial Electronics Society*. IEEE, 2018, pp. 2139–2144.

[11] A. Lizarraga, O. Begovich, and A. Ramírez, "Fault diagnosis for a three-wheel omidirectional vehicle: A geometric approach," in *2020 17th International Conference on Electrical Engineering, Computing Science and Automatic Control (CCE)*. IEEE, 2020, pp. 1–6.

[12] M. Abe, *Vehicle handling dynamics: theory and application*. Butterworth-Heinemann, 2015.

[13] K. Nam, S. Oh, H. Fujimoto, and Y. Hori, "Robust yaw stability control for electric vehicles based on active front steering control through a steer-by-wire system," *International Journal of Automotive Technology*, vol. 13, no. 7, pp. 1169–1176, 2012.

[14] H. J. Ferreau, C. Kirches, A. Potschka, H. G. Bock, and M. Diehl, "qpoases: A parametric active-set algorithm for quadratic programming," *Mathematical Programming Computation*, vol. 6, no. 4, pp. 327–363, 2014.

[15] M. Ataei, A. Khajepour, and S. Jeon, "Model predictive control for integrated lateral stability, traction/braking control, and rollover prevention of electric vehicles," *Vehicle system dynamics*, vol. 58, no. 1, pp. 49–73, 2020.